JOURNAL OF GEOPHYSICAL RESEARCH, VOL. 106, NO. A11, PAGES 25,595–25,600, NOVEMBER 1, 2001

Fast Auroral Snapshot observations of cusp electron and ion structures

Yi-Jiun Su,[1] R. E. Ergun,[1] W. K. Peterson,[2] T. G. Onsager,[3] R. Pfaff,[4] C. W. Carlson[5], and R. J. Strangeway[6]

Abstract. The high time resolution observations by the Fast Auroral Snapshot satellite resolve burst-like electrons and nonmonotonic ion dispersion in the cusp region. Electric field data from a dawn-dusk cusp crossing show that the DC electric field has small-scale variations superimposed on a large-scale pattern. The large-scale DC electric field variations are well correlated with the large-scale perturbation magnetic field, indicating a field-aligned current system that reflects a relatively homogenous conductivity. Ion structures best correlate with the perturbed magnetic field and the large-scale electric field. The burst-like precipitating electrons are correlated with the small-scale electric field variations, which are most easily explained as propagating Alfvén waves. We also found that the observed ion structures result from the spacecraft crossing the flow streamlines, each of which has its own individual history of dayside reconnection. The magnetosheath ion structures therefore contain information of both the spatial and temporal variations of dayside reconnection.

1. Introduction

In general, the cusp is a region where magnetosheath plasma of solar wind origin is injected directly into the magnetosphere and the dayside ionosphere. As observed by various spacecraft at both high and low altitudes, cusp precipitation is characterized by ion energy dispersion. During southward interplanetary magnetic field (IMF) conditions, ion energy falls with increasing magnetic latitudes, as expected, due to the convection electric field acting as a velocity filter on particles from the injection point to the observation point [i.e., *Peterson,* 1985; *Smith and Lockwood,* 1996, and references therein]. The simulation work by *Onsager et al.* [1993] has successfully reproduced the observed ion dispersion relation given by such an event. Precipitating ions, however, do not always follow a monotonic dispersion. Often complex structures, such as ion steps [e.g., *Newell and Meng,* 1991; *Escoubet et al.,* 1992], are observed. Ion steps are consistent with the effects of the temporal variation of reconnection (i.e., pulsed reconnection [*Lockwood and Smith,* 1992, 1994; *Lockwood and Davis,* 1995, 1996]) or spatial structures (i.e., patchy reconnection [*Newell and Meng,* 1991; *Onsager et al.,* 1995; *Weiss et al.,* 1995]).

Relatively few papers have discussed the behavior of the cusp electron population. Electric field observations from the Viking satellite have shown that the cusp region is characterized by irregular and burst-like electric fields [*Marklund et al.,* 1990]. *Matsuoka et al.* [1993] indicated that the irregular fluctuations of electric field observed by Exos D are considered to be Alfvén waves and suggested that the Alfvén waves are generated in association with the particle injection into the magnetosphere when reconnection occurs. *Wygant et al.* [2000] reported Polar observations of intense electric and magnetic field fluctuations associated with Alfvén waves near the outer boundary of the plasma sheet which have sufficient Poynting flux flowing along magnetic field lines toward the ionosphere to power low-altitude auroral acceleration processes.

The high time resolution observations by the Fast Auroral Snapshot (FAST) satellite reveal highly structured precipitating ions and electrons in the cusp region associated with intense electric field variations [*Pfaff et al.,* 1998]. In the following section the behavior of both precipitating ions and electrons observed by FAST is discussed. The electron structures with shorter timescale are correlated with the small-scale DC electric field, while the ion structures with longer timescale are associated with the magnetic field perturbation and large-scale electric field.

2. FAST Observations

The observations shown in this paper are from the FAST satellite electric and magnetic field instruments [*Ergun et al.,* 2001; *Elphic et al.,* 2001] and ion and electron electrostatic analyzers [*Carlson et al.,* 2001]. Data from a dawn-dusk cusp crossing in the Northern Hemisphere from 0832:30 to 0847:00 UT on July 17, 1997 (orbit 3568), are shown in Plate 1. Taking into account the time delay, the interplanetary magnetic field (IMF) observed by the Wind spacecraft was southward ($B_z < 0$) and westward ($B_y > 0$) during this time period.

In Plate 1a the perturbation magnetic fields are plotted in the spacecraft coordinate system with z along the spin axis (primarily in the direction toward the Sun), y along the spacecraft trajectory and perpendicular to $\boldsymbol{B}$ (mainly in the direction toward dusk), and x completing the orthogonal set (roughly in the direction parallel to the background magnetic field). The magnetic field perturbation was calculated from the measured magnetic field after

[1]Laboratory for Atmospheric and Space Physics, University of Colorado, Boulder, Colorado, USA.
[2]Lockheed Martin Advanced Technology Center, Palo Alto, California, USA.
[3]Space Environment Center/NOAA, Boulder, Colorado, USA.
[4]NASA/Goddard Space Flight Center, Greenbelt, Maryland, USA
[5]Space Sciences Laboratory, University of California, Berkeley, California, USA.
[6]Institute of Geophysics and Planetary Physics, University of California, Los Angeles, USA.

Paper number 2001JA000093.
0148-0227/01/2001JA000093$09.00

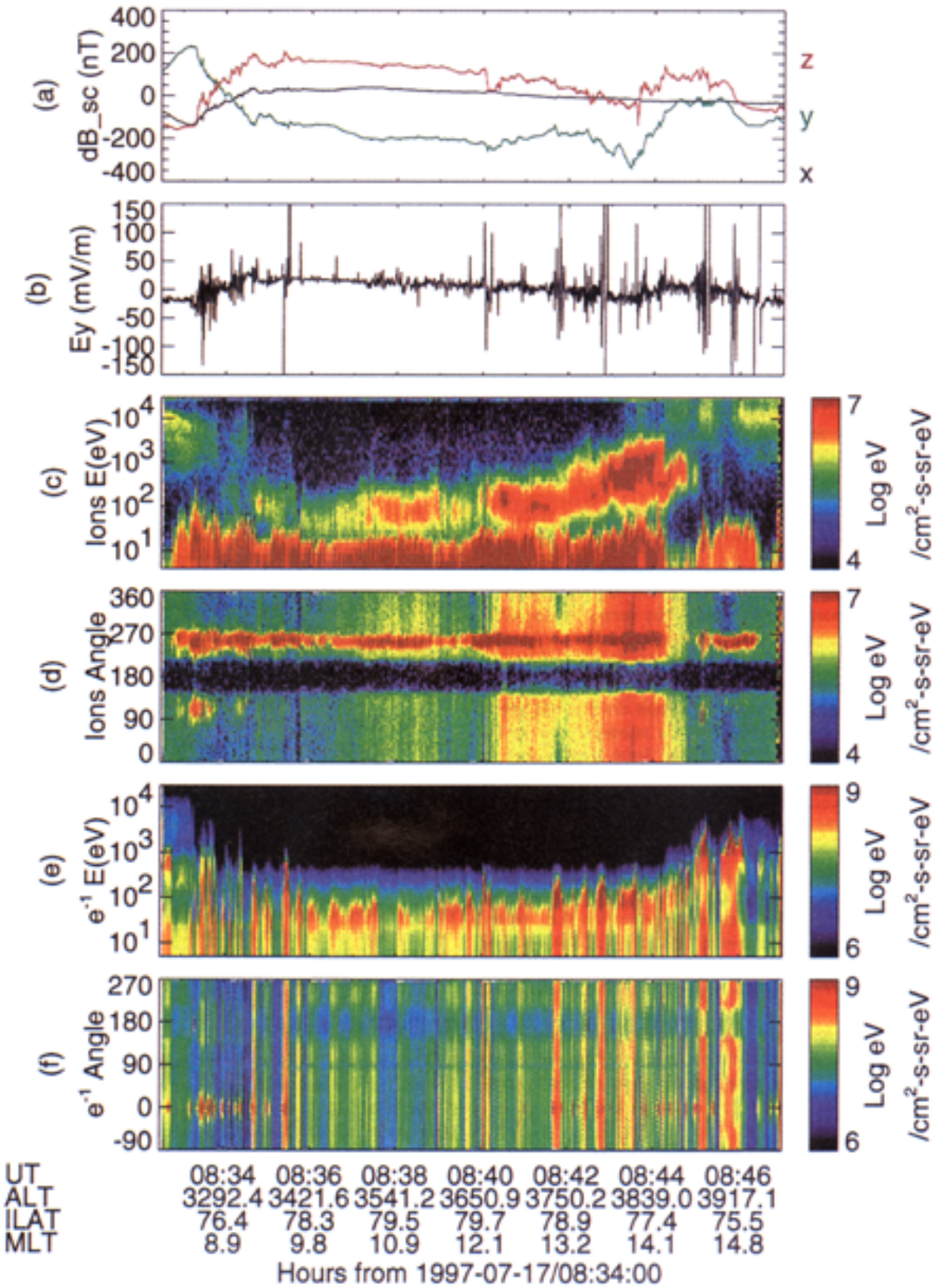

Plate 1. (a) Three components of the magnetic field perturbation, (b) DC electric field measurement perpendicular to **B** along the spacecraft track, (c) ion energy-time spectrogram, (d) ion angular spectrogram, (e) electron energy-time spectrogram, and (f) electron angular spectrogram for FAST orbit 3568 from 0832:30 to 0847:00 UT on July 17, 1997.

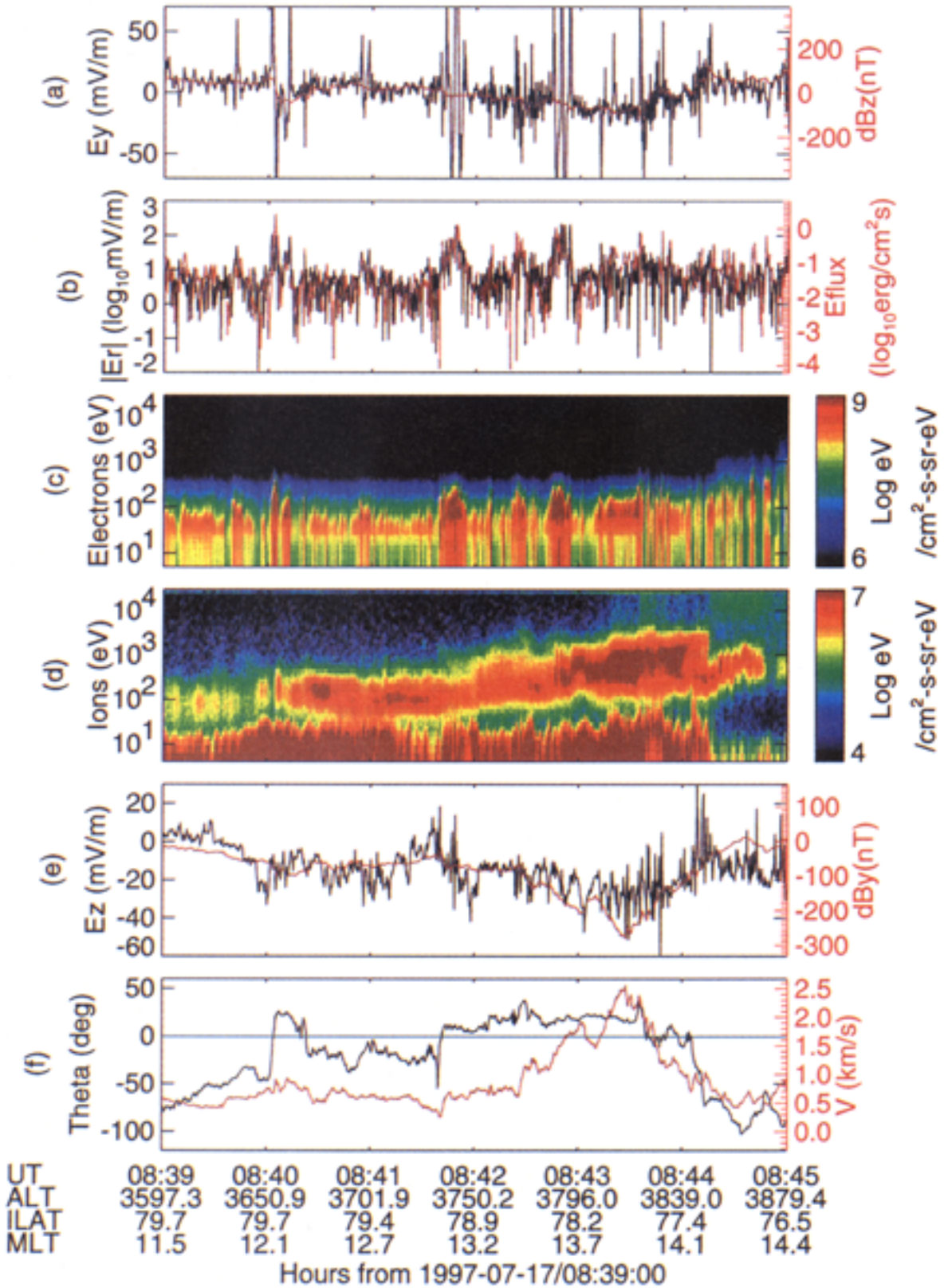

Plate 2. (a) DC electric field measurement along the spacecraft trajectory (black) and the magnetic field perturbation along the spin axis (red), (b) the absolute value of residue electric field (black) and the field-aligned electron energy flux (red) in logarithmic scale, (c) electron energy-time spectrogram, (d) ion energy-time spectrogram, (e) indirect measurement of electric field along the spin axis (black) and the perturbation magnetic field along the spacecraft trajectory (red), and (f) the directions of the drift velocities (black) where 0^{o} is along the $-y$ axis (green) and the magnitude of the drift velocities (red).

subtracting the International Geomagnetic Reference Field (IGRF) model field. In Plate 1b the measured DC electric field with maximum frequency of 1 Hz is in the direction along the spacecraft track (roughly the dawn to dusk electric field). Three distinct populations of ions can be seen in Plate 1c. (1) Plasma sheet ions with an energy of ~10 keV are present at the beginning and end of the plot, an indication that those measurements were made in the closed field line regions. (2) The ions with an energy level below ~80 eV are ionospheric conics with $\boldsymbol{E} \times \boldsymbol{B}$ drift and the spacecraft ram effect. (3) The magnetosheath ions with energies of 100s of eV are isotropic with a loss cone signature shown in Plate 1d, where 0^o and 360^o represent directions along the magnetic field line down toward the northern ionosphere. A general dispersion signature of these magnetosheath ions can be seen in Plate 1c where the ion energy increases with decreasing invariant latitude; however, this energy dispersion is not monotonic.

The electron energy-time spectrogram (Plate 1e) displays highly structured, burst-like signatures. Such signatures are often observed in the cusp region. The electron distributions are isotropic with a loss cone signature (Plate 1f). Downward electron beams can be seen in addition to the isotropic electron distribution, for instance, during 0841-0845 UT (detailed two-dimensional distribution functions are not shown here). It should be noted that upward electron beams are occasionally observed in the cusp region; however, such events are rare.

Our main focus is during the time interval from 0839 to 0845 UT. Plate 2 is an expanded view of Plate 1 from 0839 to 0845 UT. A detailed description of each panel in Plate 2 is presented in the following subsections.

2.1. E and δB

A well-documented feature of the dayside high-latitude electrodynamics is a high degree of correlation between mutually orthogonal components of the electric field and magnetic field perturbations perpendicular to the background magnetic field [cf. *Sugiura et al.,* 1982; *Sugiura,* 1984]. Such a correlation is a result of field-aligned currents flowing toward the ionosphere in a medium with relatively homogeneous conductivity. The ratio of electric field to magnetic field perturbation is given by $(\mu_o \Sigma_p)^{-1}$, where Σ_p is the height-integrated Pedersen conductivity.

From FAST observations the large-scale variations of the electric field along the spacecraft trajectory (E_y) are well correlated with the magnetic field perturbations (δB_z) along the spin axis in the cusp region. However, Plates 1a and 1b indicate that δB_z has a slightly different slope than E_y. The magnetic field perturbation was calculated from the measured magnetic field after subtracting the IGRF model field. The different slope of δB_z may be due to the neutral wind in the ionosphere and/or the selected model field. To more clearly investigate the correlated variability in the electric and magnetic fields, we have chosen to detrend the δB_z (adjusting the slope only) based on the direct measurement of E_y. The black and red lines in Plate 2a represent the direct electric field measurement (E_y) and the detrended δB_z, respectively.

As shown in Plate 2a, the observed electric field (E_y) has small-scale variations (E_r) superimposed upon a large-scale stress electric field (E_s), $E_y=E_r+E_s$. A large-scale pattern (E_s) can be seen which is well correlated with the detrended δB_z. Here E_s is obtained from a best fit of δB_z assuming a homogeneous ionospheric conductivity during the time period between 0839 and 0845 UT. A constant Pedersen conductivity is obtained to be 6.23 mhos, while an ionospheric stress velocity ($E_s/\delta B_z$) is of 127.7 km s^{-1}. It should be noted that the stress velocity is 2 orders magnitude less than the local Alfvén velocity, ~10^4 km s^{-1}. The residue electric field (E_r, small-scale variations) is then calculated by subtracting E_s from E_y. The absolute value of E_r is plotted using a logarithmic scale by the black line in Plate 2b. The small-scale variations of the electric field are believed due to the propagating Alfvén waves [*Chaston et al.,* 1999; *Matsuoka et al.,* 1993]. The large electric field spikes with amplitudes greater than 100 mV m^{-1} (for example, at ~ 0840:05, 0841:45, 0842:25, and 0842:45 UT) have been positively identified as Alfvén waves. In each wave burst, the ratio of electric field to magnetic field perturbation is the order of the local Alfvén speed. The magnetic field perturbations corresponding with smaller electric fields cannot, however, be resolved, because they are below the measurement threshold.

2.2. Electron Structures

In Plate 2c the electron energy-time spectrogram displays highly structured, burst-like signatures, which have relatively rapid variations compared with precipitating magnetosheath ions shown in Plate 2d. The burst-like electron signatures correlate well with the small-scale electric field (E_r). When a large-amplitude wave burst occurs in the electric field, an enhancement is observed in the electron energy flux as shown in the spectrogram. The red line in Plate 2b represents the field-aligned electron energy flux which can be compared with the small-scale electric field amplitude shown as the black line. The correlation coefficient between the electron energy flux (E_{flux}) and the small-scale electric field ($|E_r|$) is ~0.5. In Plate 2c a logarithmic scale was chosen to present the data in order to enhance the lesser values. We conclude that the highly irregular electron structures in the cusp are associated with the small-scale electric field fluctuations, which are associated with propagating Alfvén waves [*Chaston et al.,* 1999]. Hence Alfvén waves play an important rule in the energization of electrons. Additionally, a similar burst-like structure can been seen in the low-energy ion conics of the ion spectrogram (see Plate 2d), which suggests that Alfvén waves may be also associated with the ionospheric ion energization.

2.3. Ion Structures

In Plate 2d a general dispersion signature can be seen in the ion energy-time spectrogram, where the ion energy increases with decreasing invariant latitude; however, this energy dispersion is not monotonic. The relatively large variations in the ion energy spectrogram do not correlate with small-scale burst-like electron signatures (Plate 2c). *Weiss et al.* [1995] suggested that the step ion signature may simply represent a discontinuity in the flow velocity across the spacecraft trajectory. In order to validate this argument, we have selected a dawn-dusk crossing instead of a meridian crossing for analysis.

As shown in Figure 2 and equation (5) of *Strangeway et al.* [2000], the magnetic field perturbation is in the opposite (same) direction of the drift velocity in the Northern (Southern) Hemisphere due to the magnetic stresses. As a result of this, the flow direction can be obtained from the direction of the magnetic field perturbation. The detrended δB_z depends on the directly measured E_y shown in Plate 2a (see section 2.1). Unfortunately, no direct electric field measurement along the spin axis (E_z) exists to use as a guideline for adjusting the slope of the perturbed magnetic field along the spacecraft trajectory (δB_y). Indirectly, E_z (the black line in Plate 2e) is obtained by $V_y \times B_x$, where B_x is the main component of the background magnetic field, and V_y is obtained by the perpendicular velocity of the moment calculation

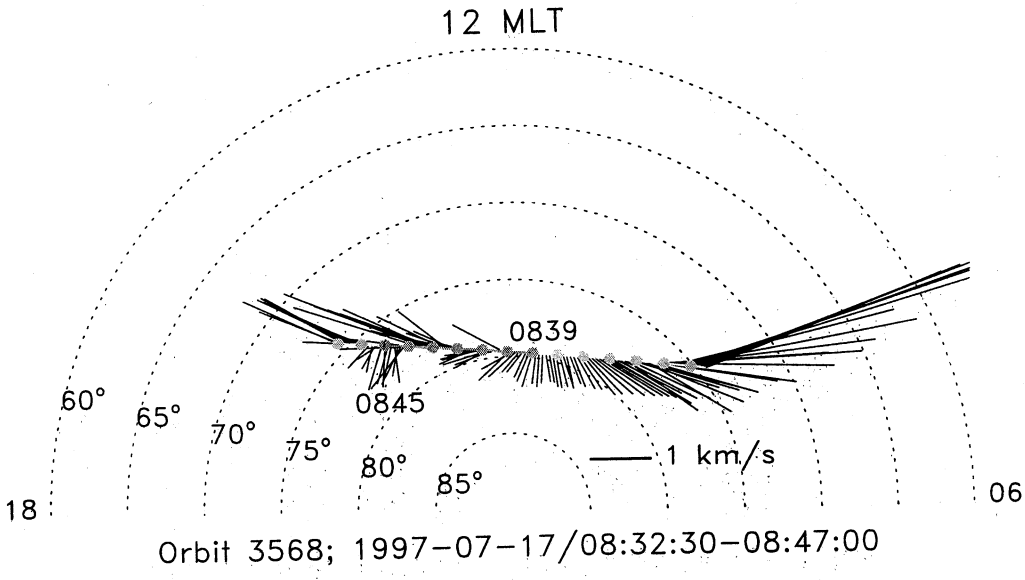

Figure 1. A polar projection of drift velocities along the spacecraft trajectory from 0832:30 (dawn) to 0847:00 UT (dusk). Each gray circle is 1 min apart, while the dark gray circles represent the same time period as that in Plate 2.

from the cold ion distribution (3 < energy < 80 eV) observed by the ion electrostatic analyzers. This method has been used successfully by *Toivanen et al.* [2001a, 2001b] on Polar observations. The magnetic field perturbation is then converted to the drift velocity in Plate 2f, where the red line represents the magnitude of flow speed and the black line represents the flow direction (0° is along -y axis in the spacecraft coordinate system). The polar projection of drift velocities is shown in Figure 1, where the gray line is the spacecraft trajectory. In this plot, each gray circle is 1 min apart, while the dark gray circles represent the same time interval as that in Plate 2.

When the IMF is southward, a well-known plasma convection exhibits a two-cell pattern with antisunward flow at the highest latitudes and return flow at lower latitudes. A typical example is shown in Figure 10 of *Lu et al.* [1989]. In general, however, the convection pattern is more complex than that. Also, the convection boundaries that exist in those empirical models [cf. *Weimer*, 1995] are smooth, whereas the instantaneous convection boundaries can be fairly sharp. As shown in our Figure 1, the flow follows a general two-cell convection pattern; however, the flow direction varies considerably at time period 0839-0845 UT. Plate 2d, Plate 2f, and Figure 1 qualitatively demonstrate that magnetosheath ion structures are associated with changing the flow direction and/or the flow speed. Hence we conclude that ion structures are due to the spacecraft crossing flow streamlines. A vortex may occur inside the large two-cell convection pattern. In addition, each flow channel has its own history associated with the dayside reconnection. For this reason, the magnitude of discontinuity in the ion energy and flux is not directly associated with the changes of the flow direction and flow speed.

Lockwood and Smith [1989] associated the cusp precipitation with flux transfer event (FTE) signatures and subsequently developed the "pulsating cusp" model [e.g., *Lockwood and Smith*, 1994]. Flow streamlines are spatial structures, because the timescale of abrupt changes in flow direction and flow speed in our study is much shorter than the mean value of recurrence rate of FTEs, 8 min, reported by *Lockwood and Wild* [1993]. Therefore a simple pulsed reconnection scenario is not sufficient to explain the nonmonotonic ion structures observed by FAST. Our result suggests a patchy reconnection at the dayside magnetopause.

3. Summary

The high timeresolution observations by the FAST satellite resolve burst-like electrons and nonmonotonic ion dispersion in the cusp region. Three dawn-dusk crossing events were examined, (1) 0835-0845 UT on July 17, 1997 (orbit 3568, which is the one presented in the paper); (2) 0728-0732 UT on July 25, 1997 (orbit 3654); and (3) 0740-0745 UT on March 21, 1998 (orbit 6241). Results similar to those described in our paper were obtained from each of these events; therefore our conclusions were not based on a unique case. The case study discussed in this paper best represents our conclusions.

Small-scale variations in the DC electric field in the cusp region are superimposed upon a large-scale pattern. The large-scale electric field is well correlated with the perturbation magnetic field orthogonal to the electric field. Moreover, the small-scale variation of the electric field is correlated with burst-like precipitating electrons. It is believed that small-scale variations are associated with propagating Alfvén waves [*Chaston et al.*, 1999]. Although Alfvén waves may play an important role in the energization of electrons, the interaction between the Alfvén waves and electrons is not completely understood.

The relatively large-scale ion structures are associated with the direction and/or magnitude of the drift velocity which is in the opposite direction of the magnetic field perturbation in the Northern Hemisphere [*Strangeway et al.*, 2000]. From this it can be concluded that magnetosheath ion structures are a result of the spacecraft crossing flow streamlines. Each flow channel has its own history of dayside reconnection. Because of this, the discontinuity in the ion spectrogram contains combined information regarding both the spatial and temporal structures of dayside reconnection. Flow streamlines (or vortices) are spatial structures; therefore a simple pulsed reconnection scenario is not sufficient to explain the magnetosheath ion structures observed by FAST. The result suggests a patchy reconnection at the magnetopause.

Acknowledgments. The authors thank the entire FAST team. This work was supported by the NASA program.

Janet G. Luhmann thanks James L. Burch and Kristina A. Lynch for their assistance in evaluating this paper.

References

Carlson, C. W., J. P. McFadden, P. Turin, D. W. Curtis, and A. Magoncelli, The electron and ion plasma experiment for FAST, *Space Sci. Rev.*, in press, 2001.

Chaston, C. C., C. W. Carlson, W. J. Peria, R. E. Ergun, and J. P. McFadden, FAST observations of inertial Alfvén waves in the dayside aurora, *Geophys. Res. Lett., 26,* 1647, 1999.

Elphic, R. C., J. D. Means, R. C. Snare, R. J. Strangeway, L. Kepko, R. E. Ergun, Magnetic field instruments for the Fast Auroral Snapshot Explorer, *Space Sci. Rev.*, in press, 2001.

Ergun, R. E., et al., The FAST satellite fields instrument, *Space Sci. Rev.*, in press, 2001.

Escoubet, C. P., M. F. Smith, S. F. Fung, P. C. Anderson, R. A. Hoffman, E. M Basinska, and J. M. Bosqued, Staircase ion signature in the polar cusp: A case study, *Geophys. Res. Lett., 17,* 1735, 1992.

Lockwood, M., and C. J. Davis, Occurrence probability, width and number of steps of cusp precipitation for fully pulsed reconnection at the dayside magnetopause, *J. Geophys. Res., 100,* 7627, 1995.

Lockwood, M., and C. J. Davis, On the longitudinal extent of magnetopause reconnection pulses, *Ann. Geophys., 14,* 865, 1996.

Lockwood, M., and M. F. Smith, Low altitude signatures of the cusp and flux transfer events, *Geophys. Res. Lett., 16,* 879, 1989.

Lockwood, M., and M. F. Smith, The variation of reconnection rate at the dayside magnetopause and cusp ion precipitation, *J. Geophys. Res., 97,* 14,841, 1992.

Lockwood, M., and M. F. Smith, Low and middle altitude cusp particle signatures for general magnetopause reconnection rate variations, 1, Theory, *J. Geophys. Res., 99,* 8531, 1994.

Lockwood, M., and M. N. Wild, On the quasi-periodic nature of magnetopause flux transfer events, *J. Geophys. Res., 98,* 5935, 1993.

Lu, G., P. H. Reiff, M. R. Hairston, R. A. Heelis, and J. L. Karty, Distribution of convection potential around the polar cap boundary as a function of the interplanetary magnetic field, *J. Geophys. Res., 94,* 13,447, 1989.

Marklund, G. T., L. G. Blomberg, C.-G. Falthammar, R. E. Erlandson, and T. A. Potemra, Signatures of the high-altitude polar cusp and dayside auroral regions as seen by the Viking electric field experiment, *J. Geophys. Res., 95,* 5767, 1990.

Matsuoka, A., K. Tsuruda, H. Hayakawa, T. Mukai, A. Nishida, T. Okada, N. Kaya, and H. Fukunishi, Electric field fluctuations and charged particle precipitation in the cusp, *J. Geophys. Res., 98,* 11,225, 1993.

Newell, P. T., and C.-I. Meng, Ion acceleration at the equatorward edge of the cusp: Low altitude observations of patchy merging, *Geophys. Res. Lett., 18,* 1829, 1991.

Onsager, T. G., C. A. Kletzing, J. B. Austin, and H. MacKiernan, Model of magnetosheath plasma in the magnetosphere: Cusp and mantle particles at low-altitudes, *Geophys. Res. Lett., 20,* 479, 1993.

Onsager, T. G., S.-W. Cheng, J. D. Perez, J. B. Austin, and L. X. Janoo, Low-altitude observations and modeling of quasi-steady magnetopause reconnection, *J. Geophys. Res., 100,* 11,831, 1995.

Peterson, W. K., Ion injection and acceleration in the polar cusp, in *The Polar Cusp,* edited by J. A. Holtet and A. Egeland, p. 67, Univ. of Oslo, Blindern, Oslo, Norway, 1985.

Pfaff, R., et al., Initial FAST observations of acceleration processes in the cusp, *Geophys. Res. Lett., 25,* 2037, 1998.

Smith, M. F., and M. Lockwood, Earth's magnetospheric cusps, *Rev. Geophys., 34,* 233, 1996.

Strangeway, R. J., C. T. Russell, C. W. Carlson, J. P. McFadden, R. E. Ergun, M. Temerin, D. M. Klumpar, W. K. Peterson, and T. E. Moore, Cusp field-aligned currents and ion outflows, *J. Geophys. Res., 105,* 21,129, 2000.

Sugiura, M., A fundamental magnetosphere-ionosphere coupling mode involving field-aligned currents as deduced from DE-2 observations, *Geophys. Res. Lett., 1,* 877, 1984.

Sugiura, M., N. C. Maynard, W. H. Farthing, J. P. Heppner, B. G. Ledley, and L. J. Cahill, Initial results on the correlation between the magnetic and electric fields observed from the DE-2 satellite in the field-aligned current regions, *Geophys. Res. Lett., 9,* 985, 1982.

Toivanen, P. K., et al., Reconciliation of the substorm onset determined on the ground and at the Polar spacecraft, *Geophys. Res. Lett., 28,* 107, 2001a.

Toivanen, P. K., D. N. Baker, W. K. Peterson, X. Li, E. F. Donovan, A. T. viljanen, A. Keiling, and J. R. Wygant, Plasma sheet dynamics observed by the POLAR spacecraft in association with substorm onsets, *J. Geophys. Res., 106,* in press, 2001b.

Weimer, D. R., Models of high-latitude electric potentials derived with a least error fit of spherical harmonic coefficients, *J. Geophys. Res., 100,* 19,595, 1995.

Weiss, L. A., P. H. Reiff, E. J. Weber, H. C. Carlson, M. Lockwood, and W. K. Peterson, Flow-aligned jets in the magnetospheric cusp: Results from the Geospace Environment Modeling Pilot program, *J. Geophys. Res., 100,* 7649, 1995.

Wygant, J. R., et al., Polar spacecraft based comparisons of intense electric fields and Poynting flux near and within the plasma sheet-tail lobe boundary to UVI images: An energy source for the aurora, *J. Geophys. Res., 105,* 18,675, 2000.

C. W. Carlson, Space Sciences Laboratory, University of California, Berkeley, CA 74920, USA.

R. E. Ergun and Y.-J. Su, Laboratory for Atmospheric and Space Physics, University of Colorado, 1234 Innovation Dr., Boulder, CO 80303, USA. (ysu@lasp.colorado.edu)

T. G. Onsager, Space Environment Center/NOAA, 325 Broadway, Boulder, CO 80303, USA.

W. K. Peterson, Lockheed Martin Advanced Technology Center, Palo Alto, CA 94304, USA.

R. Pfaff, NASA/Goddard Space Flight Center, Mail Code 696, Greenbelt, MD 20771, USA.

R. J. Strangeway, Institute of Geophysics and Planetary Physics, University of California, Los Angeles, 405 Hilgard Ave., Los Angeles, CA 90095, USA.

(Received March 28, 2001; revised May 9, 2001;
accepted May 23, 2001.)